ANALYTICAL MODELING OF AXI-SYMMETRIC SHEET METAL FORMING

Najmeddin Arab*

Faculty of Engineering, Islamic Azad University, Saveh Branch
Saveh, Iran, najarab@iau/saveh.ac.ir

Ernest Nazaryan

Faculty of Mechanics, Yerevan State University,
Armenia, nazaryan.ernest@netsys.am

*Corresponding Author

(Received: September 17, 2009 – Accepted in Revised Form: March 11, 2010)

Abstract The cup drawing is a basic deep drawing process. Thus, understanding the mechanics of the cup drawing process helps in determining the general parameters that affect the deep drawing process. There are mainly two methods of analysis; experimental and analytical/numerical. Experimental analysis can be useful in analyzing the process to determine the process parameters that produce a defect free product. However, experimental work is usually very expensive and time consuming to perform. On the other hand, the Analytical/Numerical modeling can be used to model and analyze the process through all stages of deformation. This approach is less time consuming and more economical than experimental analysis. There have been several efforts to solve and analyze the deep drawing problem. Among these are the attempts to analyze the cup drawing process, by few researches who developed analytical models for the cup drawing process to solve for stresses and strains over the deforming sheet metal. However, they did not explain how to determine the moving boundaries in the deforming sheet.. This paper deals with the analysis of deep drawing of circular blanks into axi-symmetric cylindrical cups forming using numerical modeling. A rigid plastic material model with the variational approach is used for this analysis. The amount of draw obtainable in the drawing process has been related both theoretically and experimentally with the initial diameter of the blank. The strains in the radial and circumferential directions have been measured. A correlation on the flange thickness variation by taking into account the work hardening with the analytical and experimental values also has been arrived at.

Keywords Modeling Metal Forming, Deep Drawing, Sheet Metal Forming, Analyze Thin Sheet Forming

چکیده کشش استوانه از جمله روش‌های بنیادی فرآیندهای کشش عمیق است. لذا درک درست از مکانیزم آن می‌تواندبه تعیین پارامترهای مهم این فرآیند کمک کند. اصولا دو روش تجربی و تحلیلی/ عددی برای آنالیز کشش عمیق وجود دارد. آنالیز تجربی می‌تواند در تعریف پارامتر های موثر بر تولید قطعات سالم مفید باشد. با این حال این روش‌ها غالبا پر هزینه بوده و زمان زیادی را می‌طلبند. روش‌های تحلیلی/ عددی می‌توانند برای مدل‌سازی و تحلیل فرآیند در تمامی مراحل شکل دادن به‌کار روند. این روش‌ها در مقایسه با روش‌های تجربی هزینه کمتری داشته و زمان کمتری را نیاز دارند. در سال های اخیر محققان زیادی روش مدل‌سازی تحلیلی را برای آنالیز فرآیند کشش استوانه به کار برده‌اند تا معادلات تنش– کرنش در شکل‌دادن ورق‌های نازک فلزی را حل کنند. اما اغلب این تحقیقات پدیده کار سختی و تغییرات ضخامت ورق در حین تغییر شکل را مد نظر قرار نداده یا با ارایه فرضیاتی نه چندان دقیق این فرآیند راتحلیل کرده‌اند. این مقاله کشش عمیق یک ورق استوانه‌ای به داخل قالب استوانه‌ای شکل در حالت تقارن محوری را با ارایه یک مدل تحلیلی و با در نظر گرفتن تغییرات ضخامت و کار سختی مورد مطالعه قرار داده و با استفاده از آن مقدار جدیدی را برای نسبت حد کشش ارایه داده است.

1. INTRODUCTION

The production of high quality formed products in a short time and at a low cost is an ultimate goal in manufacturing. To reach this goal, continuous

rogress are made at the design and at the floor shop levels of forming process [1]. The stage of research and development in CAD/CAM/CAE in relation with the analysis and design of forming parts can be observed from several papers published in roceedings of international meetings [2,3].

To avoid trial and error tryout procedures, the sheet metal forming simulation is increasingly being used in the stamping industry to evaluate the deformation paths and the forming defects such as fracture and wrinkling. Many research groups are still developing and improving finite element codes for the analysis when an initial design of the blank and the tools is done and when the forming conditions are defined. Several analysis tools are described in the proceedings [2,3].

They are based on membrane, shell or even solid elements, considering static or dynamic, implicit or explicit approaches. These analysis tools can be very precise if used by well-trained engineers, but they are time consuming and need expensive computer resources. Computersimulation can also be very attractive and helpful for theprocess and tooling engineers to define the initial blank (thickness, contour and surface), some process parameters (boundary conditions, holding forces, lubrication conditions, drawbead types and positions, etc.) and the material properties (yield stress, hardening, anisotropy, etc.). This has been recognized by some industrial and academic research and development groups. As a result a number of methods have been developed in the last decade. They are mainly based on the fact that the shape of the desired part is known. A comparison is then made with the initial flat blank to estimate the deformation of the final product taking in to account simple constitutive equations and assumptions regarding the tool actions. These simplified procedures have been called different names: 'geometrical mapping method' [4], 'single and multi-stage forming formulations' [5], 'one step solution' [6], 'ideal forming theory' [7], 'inverse approach' (IA) [8–12] and 'simplified approach' [13].

The inverse approach is based on a discretization of the final workpiece by simple triangular flat facet shell elements.

For a large number of industrial applications, the membrane effects are dominant, but it has been necessary to consider bending effects using a simple discrete Kirchhoff shell element [14–16].

Assumptions were made regarding the action of the tools (punch and die) at the end of the forming process.

Logarithmic strains and total deformation theory of plasticity were considered. The equilibrium of the workpiece leads to a set of nonlinear equations. These nonlinear equations can be solved by different techniques such as the Newton–Raphson static implicit approach, the dynamic relaxation method or the dynamic explicit algorithm [17–21]. The convergence difficulties can be encountered for practical situations involving deep drawing workpieces (with almost vertical walls) and a low plastic hardening law. A simplified scheme in order to estimate the trimming part of the workpiece for a given blank shape, flat or curved has been developed. The inverse approach has been continuously evaluated by comparing the numerical results with experimental and other numerical results obtained by incremental approaches. The procedure has been found very efficient and quite precise at the preliminary tool design stage [22-23]. Based on the

ideas of the simplified inverse approach two industrial codes have been developed [24-26]. The codes are routinely used at the preliminary forming design stage of car panels and thin walled structural members. Some backwards simulation codes have been developed and used in the industry[27-29].

In this paper, in order to increase the efficiency and accuracy of the modeling procedure, the yielding criteria and radial and circumference strains among with strain hardening and thickness variations during the forming process has been employed. Finally optimum results are obtained and presented and discussed.

2. SHEET METAL FRMING AT AXI-SYMMETRIC CONDITION

At axi-symmetric condition the forming of sheet metal occurs in plane stress state [30-32]. Stress and strain can be defined by the joint solution of the equations of plasticity theory and the equation describing deformation hardening [30].

According to Mises' yield criteria, yield stress

calculated as

$$\sigma_s = \{\frac{1}{2}[(\sigma_\rho - \sigma_\theta)^2 + (\sigma_\theta - \sigma_z)^2 + (\sigma_z - \sigma_\rho)^2]\}^{1/2}. \quad (1)$$

$\sigma_\rho, \sigma_\theta, \sigma_z$ - are the main stresses in radial, circular and thickness direction respectively.

Yield stress in quation (1) depends on the value of effective strain which is defined as:

$$\varepsilon_i = \{\frac{2}{9}[(\varepsilon_\rho - \varepsilon_\theta)^2 + (\varepsilon_\theta - \varepsilon_z)^2 + (\varepsilon_z - \varepsilon_\rho)^2]\}^{1/2} \quad (2)$$

$\varepsilon_\rho, \varepsilon_\theta, \varepsilon_3$ - are the main strains in the same directions, satisfying the condition of volume constancy

$$\varepsilon_\rho + \varepsilon_\theta + \varepsilon_z = 0 \quad (3)$$

Relationship between stresses and main strains is as follow

$$\frac{d\varepsilon_\rho - d\varepsilon_\theta}{\sigma_\rho - \sigma_\theta} = \frac{d\varepsilon_\theta - d\varepsilon_z}{\sigma_\theta - \sigma_z} = \frac{d\varepsilon_z - d\varepsilon_\rho}{\sigma_z - \sigma_\rho} = \frac{3}{2}\frac{d\varepsilon_i}{\sigma_s} \quad (4)$$

$d\varepsilon_i$ - is the intensity of increment of main strains which is defined as follow

$$d\varepsilon_i = \{\frac{2}{9}[(d\varepsilon_\rho - d\varepsilon_\theta)^2 + (d\varepsilon_\theta - d\varepsilon_z)^2 + (d\varepsilon_z - d\varepsilon_\rho)^2]\}^{1/2}. \quad (5)$$

In the conditions of plane stress state $(\sigma_z = 0)$ it follows from equation (4)

$$d\varepsilon_\rho = \frac{2\sigma_\rho - \sigma_\theta}{2\sigma_\theta - \sigma_\rho} d\varepsilon_\theta, \quad d\varepsilon_z = \frac{\sigma_\rho + \sigma_\theta}{\sigma_\rho - 2\sigma_\theta} d\varepsilon_\theta. \quad (6)$$

It is convenient to present the dependence between the yield stress (1) and the effective strain in the form of following function [31-32]

$$\sigma_s = A\varepsilon_i^n, \quad (7)$$

A, n - are the parameters of deformation hardening depending on mechanical properties of the sheet metal.

The equilibrium equation which has been cut out by the main sections from axi-symmetrically loaded cover of variable thickness looks like [30]

$$\rho\frac{d\sigma}{d\rho} + \sigma_\rho(1 + \frac{\rho\, ds}{s\, d\rho}) - \sigma_\theta = 0. \quad (8)$$

Increments of the main strains in circular direction and in the direction of thickness are connected with the increment of radius $d\rho$ and thickness ds with parities

$$d\varepsilon_\theta = \frac{d\rho}{\rho}, \quad d\varepsilon_z = \frac{ds}{s}. \quad (9)$$

Substituting (9) in (8), taking into account dependences (6), after substitution it shall obtain

$$\rho\frac{d\sigma_\rho}{d\rho} + 2\frac{\sigma_\rho^2 - \sigma_\rho\sigma_\theta + \sigma_\theta^2}{2\sigma_\theta - \sigma_\rho} = 0 \quad (10)$$

Taking into account (1) integration (10) is possible only for ideal plastic model of deformable material $(\sigma_s = const)$. When integrating (10) with deformation hardening, acceptance of the further simplifications is necessary, basis of them is the condition of thickness constancy. Such assumption is equivalent to the statement that sheet metal forming occurs in the conditions of plane strain basically excluding the possibility of solution to the problems in which plane stress state is realized.

3. STRAIN AND STRESS AT PLANE STRESS CONDITION AND THEIR RELATION

It follows from condition (3) that in case of large plastic deformations, strains are interconnected and can be presented on the plane in oblique-angled coordinates. Let's consider π - plane of plasticity cylinder where the point of origin corresponds to zero strain (blank before deformation), and the locus of points of consecutive deformed conditions represents a way of deformation of the considered point particle. Generally current values of main stress represent projections of vector-function $\vec{\varepsilon}_i$ on oblique-angled coordinate axes, the deformation procedure is described by vector function $\vec{\varepsilon}_i(\rho)$ (ρ - some time parameter), and the direction of deformation speed $d\vec{\varepsilon}_i / d\rho$ coincides with the tangent of deformation path. The module of current size of vector function $\vec{\varepsilon}_i(\rho)$ numerically equals the equivalent strain (2) [33].

In the considered plane it is convenient to present increments of the main strains in trigonometrically form:

$$d\varepsilon_\rho = d\varepsilon_i \cos\varphi, \quad d\varepsilon_\theta = d\varepsilon_i \cos(\varphi + \frac{2}{3}\pi),$$
$$d\varepsilon_z = d\varepsilon_i \cos(\varphi + \frac{4}{3}\pi), \tag{11}$$

φ - is the angle of the kind of deformed condition.

From the joint decision of (6) and (11) depending on radial and circular stresses on the angle of the kind of deformed condition the following equations are established:

$$\sigma_\rho = \sigma_s \frac{2}{\sqrt{3}} \cos(\varphi + \pi/6), \sigma_\theta = -\sigma_s \frac{2}{\sqrt{3}} \sin\varphi \tag{12}$$

These equations satisfy Mises' yield criterion For simplification of interpretation of the received results the reference point on π - plane is combined with axis ε_ρ, and the increase in angle φ is taken in the direction counter-clockwise. At change $0 \le \varphi \le 2\pi$ radial beams divide π - plane into 12 sectors with the central angles equal $\pi/6$ (Figure 1 a).

In the specified change range of parameter φ vector function $\vec{\varepsilon}_i(\rho)$ becomes either parallel, or perpendicular to coordinate axes $\varepsilon_\rho, \varepsilon_\theta, \varepsilon_z$ owing to what the main strains on these axes change within limits from one to zero.

Taking into account equation (10) it is possible to present (11) and (12) equation of equilibrium π - plane in quite a simple way

$$d\sigma_\rho = \sigma_s d\varepsilon_i \ . \tag{13}$$

Thus, the system of equations characterizing plane stress state is displayed on π -plane in the form of linear dependence between speeds of change of radial stress and equivalent strain. Proportionality constant in (13) is yield stress of the material, characterizing, according to (7), deformation hardening.

assuming $d\varepsilon_i = |d\varepsilon_\theta|$ and using yield criterion $\sigma_\rho - \sigma_\theta = \sigma_s$ differential equation(13)becomes:

$$\rho \frac{d\sigma_\rho}{d\rho} + \sigma_\rho - \sigma_\theta = 0,$$ which represents

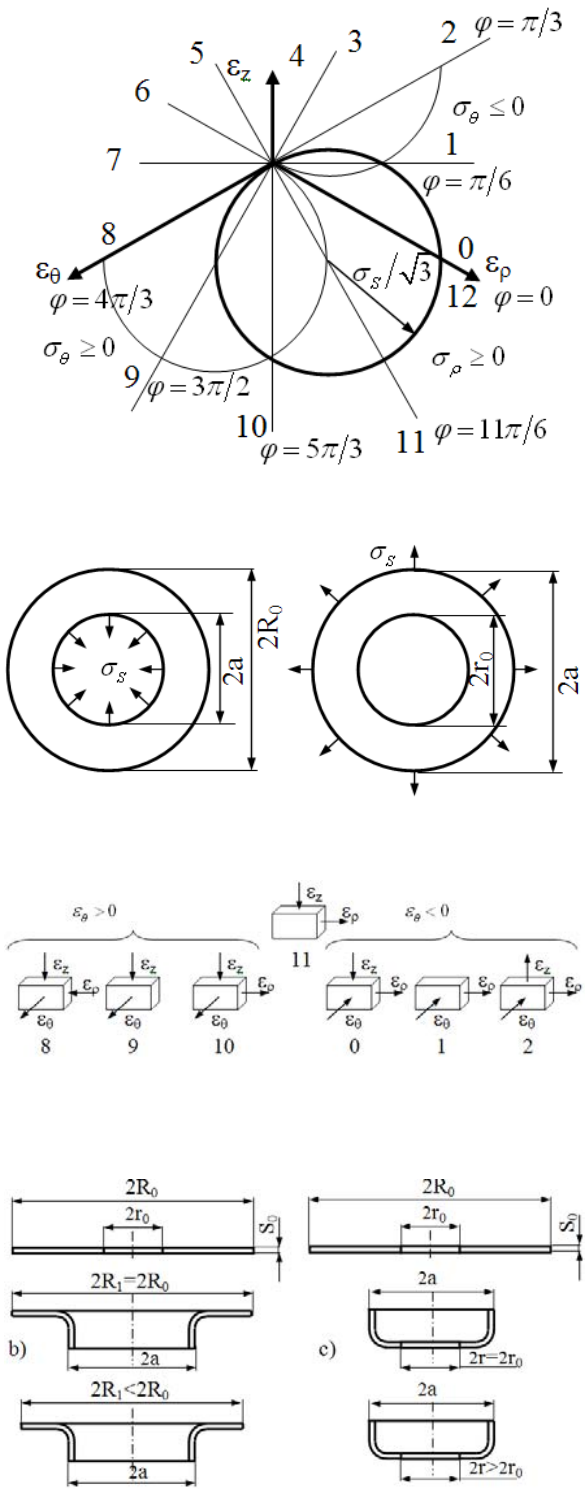

Figure 1. Stress condition on π -plane (a) and deformation types (b-flanging, c-drawing)

equilibrium equation usually applied in researches without change of thickness.

4. ANALYSIS OF THIN RING PLATES DEFORMATION

Let's consider thin ring plate having the sizes R_0, r_0, s_0. At certain dimensional characteristics of the plate and forming tool the following variants of forming are possible [34]:

- drawing cylindrical cup at constant or variable value of diameter of the central hole (Figure 1 c).
- Flanging central hole at constant or variable value of diameter of an external contour (Figure 1 b).

The given character of forming allows us to conventionally divide deformation of ring plate into two components: stretching of ring plates with the sizes R_0, a, s_0 and a, r_0, s_0 under the yield stress σ_s accordingly applied to internal and to external contours. It is obvious that at such condition the stresses arising due to material bending on radial flanges of deforming tools are not taken into consideration, and the size of the ring dividing the drawing zone from flanging zone is replaced with conventional circle with radius a.

The problem with integration (13) that generally the increment of equivalent strain defined by differentiation (2) does not equal increment intensity of the main strain(5). It is easy to show that such equality is possible only at proportional change of main strains that corresponds to radial ways of deformations on π - plane.

Considering this assumption it follows from (13):

$$\sigma_\rho = \frac{A}{n+1}\varepsilon_i^{n+1} + c \ . \tag{14}$$

Integration constant is found from boundary conditions on which for contours free from load radial stresses equal zero. Taking into account boundary conditions and by equating the integration result to equation (12), we will have

$$\varepsilon_i^{n+1} - \varepsilon_{kp}^{n+1} = (1+n)\varepsilon_i^n \frac{2}{\sqrt{3}}\cos(\varphi + \pi/6) \ . \tag{15}$$

Change limits for angle of deformation state kind in the considered problems are established depending on the sign of circular deformation and the value of the greatest stretching stresses. From equation (12) follows that in directions $\varphi = 0$, $\varphi = 5\pi/3$ radial stresses reach the size equal to material yield point. Whereas in the range of angles $0 \le \varphi \le \pi/3$ circular strains are negative, and in range $4\pi/3 \le \varphi \le 5\pi/3$ these strains are positive. Thus, all kinds of strains which basically can be realized in drawing and flanging processes are situated on half-plane and occupy equal sectors with central angles $\varphi = \pi/3$ (Figure 1 a).

If deformation path coincides with axis ε_θ, then stretching strain is ε_θ in.

The received solution allows establishing interrelation between coordinates of the considered material parameters and the angle of deformation state kind. For this purpose, by differentiating (15) at $\varepsilon_{kp} = 0$, and taking into account (9), (11), result

$$\frac{d\rho}{\rho} = (1+n)\cdot\left(\sin\varphi\cos\varphi + \frac{\sqrt{3}}{2}\sin^2\varphi + \frac{\sqrt{3}}{6}\cos^2\varphi\right)d\varphi \cdot$$

After integration (16) results in

$$\ln\rho = (1+n)\cdot\left(\frac{\sqrt{3}}{3} - \frac{1}{4}\cos 2\varphi - \frac{\sqrt{3}}{12}\sin 2\varphi\right) + C \ . \tag{17}$$

The integration constant in (17) is obtained from the following boundary conditions: for external ring plate $\rho = R_0$, $\varphi = \pi/3$; for internal ring plate $\rho = r_0$, $\varphi = 4\pi/3$. Taking into account boundary conditions expression (17) becomes for external ring plate

$$\frac{\rho}{R_0} = \exp\left[(1+n)\cdot\left(\frac{\sqrt{3}}{3}(\varphi - \pi/3) - \frac{1}{4}\cos 2\varphi - \frac{\sqrt{3}}{12}\sin 2\varphi\right)\right] \tag{18}$$

for internal ring plate

$$\frac{\rho}{r_0} = \exp\left[(1+n)\cdot\left(\frac{\sqrt{3}}{3}(\varphi - 4\pi/3) - \frac{1}{4}\cos 2\varphi - \frac{\sqrt{3}}{12}\sin 2\varphi\right)\right] \tag{19}$$

Substituting in (18) and (19) the limiting values of

angles of deformation state kind $\varphi = 0,\ \varphi = \frac{5}{3}\pi$ at which stretching stresses reach the value equal to material yield point, we will receive the relation of the greatest sizes of ring plates

$$\frac{a}{r_0} = \frac{R_0}{a} = \exp\left[(1+n)\cdot\left(\frac{1}{4}+\frac{\sqrt{3}\pi}{9}\right)\right] \approx \exp\left[0{,}854\cdot(1+n)\right] \tag{20}$$

At $n = 0$ limiting values of relations R_0 / a and a / r_0 (Limit Drawing Ration (LDR)) are equal to 2.35 which coincides with the result of work [4] and is close enough to the values usually seen in experiments [35-37]. Using value of equivalent strain, it is easy to define the main strains for the initial plastic state of ring plates:

$$\begin{aligned}
\varepsilon_\rho &= \frac{1+n}{2}\left(1+\cos 2\varphi - \frac{\sqrt{3}}{3}\sin 2\varphi\right)\\
\varepsilon_\theta &= -\frac{1+n}{2}\left(\cos 2\varphi + \frac{\sqrt{3}}{3}\sin 2\varphi\right)\\
\varepsilon_z &= -\frac{1+n}{2}\left(1-\frac{2\sqrt{3}}{3}\sin 2\varphi\right)
\end{aligned} \tag{21}$$

Thus, interdependence among (12), (15), (18), (19) and (21), being the parametrical solution of the problem, completely define the stress-strain state of ring plates taking into account the interconnected change of material thickness and deformation hardening.It is obvious that by eliminating parameter φ it is possible to obtain the interdependences characterizing the distribution of main stresses and strains on coordinate of material parameters for the initial plastic states of plates.

5. RESULTS & DISCUSSION

On Figure 2 a, b the distribution graphs of equivalent and main strains are presented, and on Figure 2 c, d the distribution graphs of main stresses and thickness for internal and external ring plates, are accordingly presented.

From graphs some characteristic features of forming ring plates follow. For external ring plate equivalent strain and radial component differ slightly. On the boundary area the external plate experiences thickening deformation, and absolute value of circular deformation at some distance from the internal contour reaches its maximum.

For internal ring plate equivalent strain and deformation by thickness slightly differ in absolute value. At internal contour the internal plate undergoes deformation of radial compression, and circular deformation at some distance from external contour reaches its maximum. Deformation hardening, not changing the deformed state in quality, essentially influences the stress state. Coordinates of material parameters, which limit characteristic kinds of deformation, may be defined from equations (18), (19).

The determined distribution of strains may be used both for definition of the initial sizes of ring plates on the set sizes of the blank and for optimization of parameters of the forming process.

(21)

6. CONCLUSIONS

1. Analytical solution of the problem of thin ring plates forming for biaxial homogenic and heterogenic stress state was studied by considering the changes in material thickness and deformation hardening.
2. It was established that the limit drawing ratio for real plastic deformation of the material which has variation of thickness and work hardening during the forming stage is 2.35.
3. It was shown that deformation hardening not changing the deformation state in quality, essentially influences the stress state.
4. The results of the present analytical model showed good agreement with experimental results.
5. The present model can be useful in conducting parametric studies on different parameters affecting the process, including die design, process and material parameters.
6. The present analytical model lends itself as an analysis tool for the design of any cup drawing process. It can be used as a fast procedure to perform a preliminary analysis to predict the stresses and strains induced in the forming cup and to determine the suitable parameters that give the least strains.

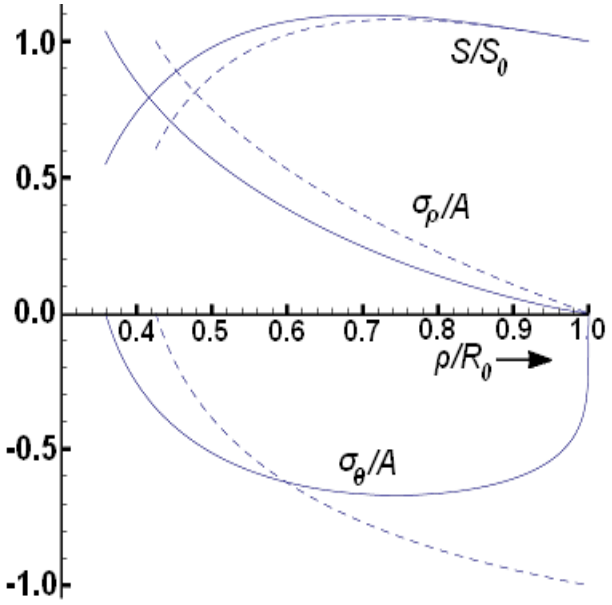

(a)

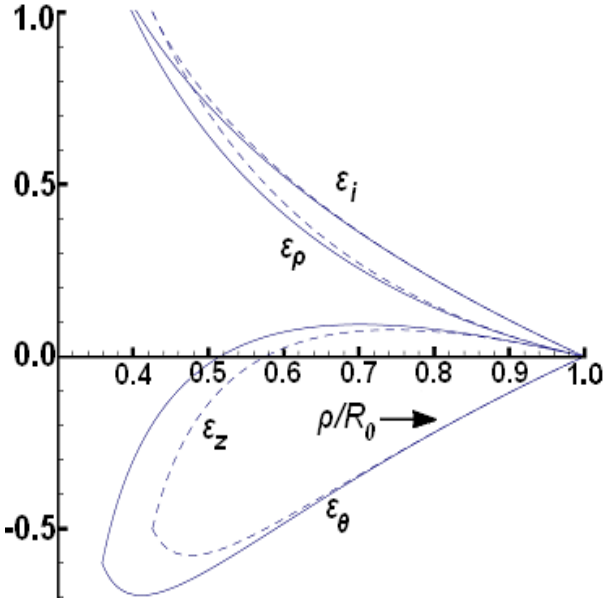

(c)

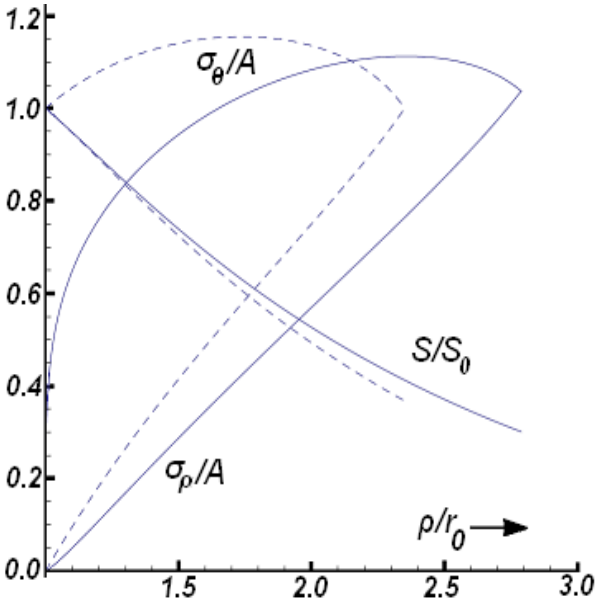

(b)

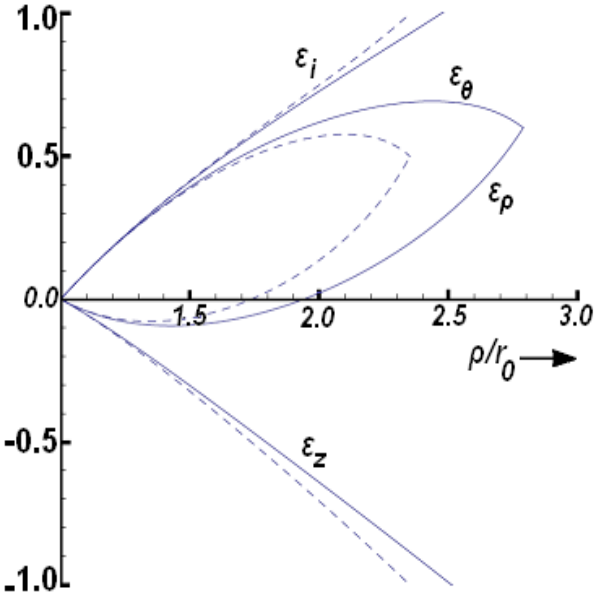

(d)

Figure 2. The distribution of main stresses and thickness (a,b) and equivalent main strains for external and internal ring plates (c,d) (----n=0; ___ n=0.2).

7. ACKNOWLEDGEMENTS

The authors wish to thank professor V. Sarkisyan, professor B. Balasanyan and professor G.L. Petrosyan, and professor S. Aghbalyan for supporting and supervising this research.

8. REFERENCES

1. H. Sattari, , R. Sedaghati, R. Ganesan, Analysis and design optimization of deep drawing process. Part 1. Three dimensional finite element and sensitivity analysis, ***J. Mater. Process. Technol***., vol 184, 2007, pp 84-92.
2. B. Kroplin, E. Luckey (Eds.), Metal forming process simulation in industry, in: International Conference and Workshop, Baden-Baden, Germany, 28– 30, 1994.
3. J.K. Lee, G.L. Kinzel, R.Wagoner, Numerical simulation of 3D sheet metal forming processes, verification of simulations with experiments, in: Third International Conference on NUMISHEET 96, the Ohio State University, Dearborn, MI, September 29–October, 1994.
4. J.C. Gerdeen, P. Chen, Geometric mapping method of computer modeling of sheet metal forming, NUMISHEET 89 (1989) 437–444.
5. K. Chung, D. Lee, Computer-aided analysis of sheet material forming processes, ***First International Conference on Technology of Plasticity***, vol. 1, Tokyo, Japan, 1984, pp. 660–665.
6. M.P. Sklad, B.A. Yungblud, Analysis of multi-operation sheet forming processes, ***NUMISHEET*** 92 (1992) 543–547.
7. K. Chung, O. Richmond, Sheet forming process design on ideal forming theory, ***NUMISHEET*** 92 (1992) 455–460.
8. J.L. Batoz, P. Duroux, Y.Q. Guo, J.M. Detraux, An efficient algorithm to estimate the large strains in deep drawing, ***NUMISHEET*** 89 (1989), pp 383–388.
9. J.L. Batoz, H. Naceur, O. Barlet, Y.Q. Guo, C. Knopf-Lenoir, Optimum design of blank contours in axisymmetrical deep drawing process, in: Z. Wan-Xie, C. Geng-dong, Xi-Kui Li (Eds.), Advances in Computational Mechanics, ***International Academic Publisher***, Beijing, China, 1996, pp. 113–125.
10. Y.Q. Guo, J.L. Batoz, H. Naceur, S. Bouabdallah, F. Mercier, O. Barlet, Recent developments on the analysis and optimum design of sheet metal forming parts using a simplified inverse approach, Comput. Struct. 78 (2000) 133–148.
11. H. Naceur, A. Delam´eziere, J.L. Batoz, Y.Q. Guo, C. Knopf-Lenoir, Some improvements on the optimum process design in deep drawing using the inverse approach, ***J. Mater. Process. Technol***. 146 (2) (2004) 250– 262.
12. O. Barlet, J.-L. Batoz, Y.Q. Guo, F. Mercier, H. Naceur, C. Knopf-Lenoir, The inverse approach and mathematical programming techniques for optimum design of sheet forming parts, ESDA 96', 3rd. Biennial European Joint Conference on Engineering Systems Design and Analysis, Montpellier, France, July 1–4, 1996. © ASME 1996, PD-vol. 75, Eng. Syst. Des. Anal. Vol. 3, pp. 227–232.
13. X. Chateau, A simplified approach for sheet forming processes design, ***Int. J. Mech. Sci***. 36 (6) (1994) 579–597.
14. G. Dhatt, G. Touzot, S.A. Maloine (Eds.), Une pr´esentation de la m´ethode des ´el´ements finis, L'Universit´e Laval Qu´ebec, Paris, 1981.
15. J.L. Batoz, G. Dhatt, Mod´elisation des structures par ´el´ements finis, vol. 3, Coques, Ed. Herm`es, Paris, 1992.
16. E. O˜nate, M. Kleiber, C. Agelet de Saracibar, Plastic and viscoplastic flow of void-containing metals. Applications to axisymmetric sheet forming problems, ***Int. J. Numer. Methods Eng***. 25 (1988) 227–251.
17. H. Matthies, G. Strang, The solution of nonlinear finite element equations, ***Int. J. Numer. Methods Eng***. 14 (1979) 1613–1626.
18. D.R.J. Owen, E. Hinton, Finite elements in Plasticity: Theory and Practice, Pineridge press, Swansea, 1980.
19. D. Peric, D.R.J. Owen, M.E. Honnor, Simulation of thin sheet metal forming processes employing a thin shell element. FE simulation of 3-D sheet metal forming processes in automotive industry, ***VDI Verlag, Z¨urich***, pp.569–600, 1991.
20. H.D. Hibbitt, P.V. Marcal, J.R. Rice, A finite element formulation for problems of large strain and large displacement, ***Int. J. Solids Struct***. 6 (1970)1069–1086.
21. R.M. McMeeking, J.R. Rice, Finite-element formulations for problems of large elastic-plastic deformation, ***Int. J. Solids Struct***. 11 (1975) 601–616.
22. K. Washizu, Variational Methods in Elasticity and Plasticity, third ed., Pergamon, Oxford, 1982.
23. E.H. Lee, Elastic-plastic deformation at finite strains, ***J. Appl. Mech***. 36 (1969) 1–6.
24. T.J. Chung, Continuum Mechanics, Prentice Hall, New Jersey, 1988.
25. J.S. Arora, Introduction to Optimum Design, McGraw-Hill Book Company,1989.
26. G.N.Vanderplaats,Numerical Optimization Techniques for Engineering Design With Applications, McGraw-Hill Inc., 1984.
27. B.H.V. Topping, D.J. Robinson, Selecting non-linear optimization techniquesfor structural design, Intl. J. Comput. Aided Eng. Software Eng. Comput. 1 (3) (1984).
28. B. Prasad, R.T. Haftka, Optimal structural design with plate finite elements, ASCE, J. Struct. Div. 105 (ST11) (1979).
29. E. Rohan, J.R. Whiteman, Shape optimization of elasto-plastic structures and continua, Comput. ***Methods Appl. Mech. Eng***. (2000).
30. E. Popov: "Foundations of Sheet Metal Forming Theory", Moscow, Machine-building (1977) pp 278.
31. Z. Marciniak, J. Dunkan, S. Hu: "Mechanics of Sheet Metal Forming", published by ***Butterworth-Heinemann***

(2002) 205.
32. R. Hill: “The Mathematical Theory of Plasticity”, Oxford Classic Texts (1998) 362.
33. E. Nazaryan, V. Konstantinov, “Kinematics of Straining in Deformation Operations of Sheet Stamping”, Moscow, Bulletin of Machine-building 2 (1999) 35-41.
34. E. Nazaryan, N. Arab," Deformation at Flanging Circular Holes in Thin Plates", ***Journal of Blanking Production in Mechanical Engineering***, No. 3, March 2009,pp 22-26.
35. M. Berger, E. Zussman, "On-Line Thinning Measurment in Deep Drawing Process", ***Journal of Manufacturing Science and Engineering***, Vol 124, May 2002, pp.420-425.
36. H. Satari, R. Sedaghati, R. Ganesan, "Analysis and Design Optimization of Deep Drawing Process, Pat I , II", ***Journal of Materials Processing Technology***, Vol. 184, 2007, pp 84-92.
37. C. Garcia, D. Celentano, et. al, "Numerical Modeling and Experimental Validation of Steel Deep Drawing Process, Part I , II", ***Journal of Materials Processing Technology***, Vol. 172, pp. 461- 471.